Optical properties of $LiGaS_2$: an *ab initio* study and spectroscopic ellipsometry measurement

2009 J. Phys.: Condens. Matter 21 455502

(http://iopscience.iop.org/0953-8984/21/45/455502)

J. Phys.: Condens. Matter **21** (2009) 455502 (5pp) doi:10.1088/0953-8984/21/45/455502

Optical properties of $LiGaS_2$: an *ab initio* study and spectroscopic ellipsometry measurement

V V Atuchin[1], Z S Lin[2,6], L I Isaenko[3], V G Kesler[4], V N Kruchinin[5] and S I Lobanov[3]

[1] Laboratory of Optical Materials and Structures, Institute of Semiconductor Physics, SB RAS, Novosibirsk 90, 630090, Russia
[2] Beijing Center for Crystal R&D, Technical Institute of Physics and Chemistry, Chinese Academy of Sciences, PO Box 2711, Beijing 100190, People's Republic of China
[3] Laboratory of Crystal Growth, Institute of Geology and Mineralogy, SB RAS, Novosibirsk 90, 630090, Russia
[4] Laboratory of Physical Bases of Integrated Microelectronics, Institute of Semiconductor Physics, SB RAS, Novosibirsk 90, 630090, Russia
[5] Laboratory for Ellipsometry of Semiconductor Materials and Structures, Institute of Semiconductor Physics, SB RAS, Novosibirsk 90, 630090, Russia

E-mail: zslin@mail.ipc.ac.cn

Received 4 August 2009, in final form 16 October 2009
Published 23 October 2009
Online at stacks.iop.org/JPhysCM/21/455502

Abstract

Electronic and optical properties of lithium thiogallate crystal, $LiGaS_2$, have been investigated by both experimental and theoretical methods. The plane-wave pseudopotential method based on DFT theory has been used for band structure calculations. The electronic parameters of Ga 3d orbitals have been corrected by the DFT + U methods to be consistent with those measured with x-ray photoemission spectroscopy. Evolution of optical constants of $LiGaS_2$ over a wide spectral range was determined by developed first-principles theory and dispersion curves were compared with optical parameters defined by spectroscopic ellipsometry in the photon energy range 1.2–5.0 eV. Good agreement has been achieved between theoretical and experimental results.

(Some figures in this article are in colour only in the electronic version)

1. Introduction

There is considerable interest in new effective nonlinear optical crystals applicable for frequency conversion over a wide spectral range, from visible to infrared (IR). This relentless activity is motivated by the development of coherent parametric down-conversion sources promising for numerous applications in environmental control, microelectronics and nanotechnology. Well-studied oxide nonlinear optical materials are typically not transparent at wavelengths $\lambda \geqslant 5$–7 μm because of fundamental properties of oxide chemical bonds. So, other compounds related to different chemical classes, in particular sulfides and selenides, should be considered in searching for nonlinear materials transparent in the IR spectral region.

Lithium thiogallate $LiGaS_2$ (LGS) is a noncentrosymmetric crystal, space group $Pna2_1$, $a = 6.5133(6)$ Å, $b = 7.8629(8)$ Å, $c = 6.2175(5)$ Å, $Z = 4$, with appropriate birefringence and relatively high nonlinear optical coefficients beneficial for effective optical frequency conversion [1–3]. The crystal structure of LGS is presented in figure 1. Each gallium atom is four-coordinated with neighboring sulfur atoms to form the GaS_4 tetrahedron and lithium atoms are located in the cavity surrounded by the GaS backbone. LGS is transparent over a very wide spectral range $\lambda = 0.32$–11.6 μm at the 5 cm^{-1} level [2] and is a representative member of the broad family of isostructural compounds $LiMX_2$ (M = Al, In, Ga; X = S, Se, Te), whose properties can be continuously tuned by solid

[6] Author to whom any correspondence should be addressed.

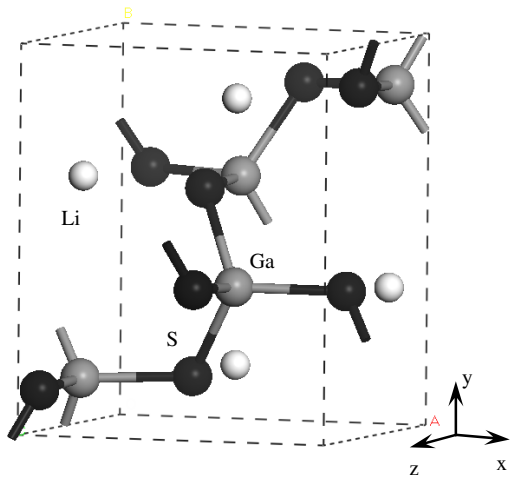

Figure 1. Unit cell of $LiGaS_2$. The white, gray and black circles represent lithium, gallium and sulfur atoms, respectively.

solution formation [3, 4]. Following recent efforts in crystal growth methods, high quality LGS crystals are now available for the creation of frequency conversion devices [3, 5, 6].

It would be very valuable to see the nature of unusual optical properties of LGS, in particular, a very wide transparency range and noticeable birefringence, and relate crystal properties to specific features of chemical bonding in this binary sulfide. Presently known empirical relations are only able to give some general predictions for the physical properties of sulfide crystals [7–11]. As a rule the relations are simple and are based on local functional units of a compound. On the other hand, more detailed analysis is possible by using first-principles calculations starting directly from available crystal structure data and chemical composition [12–15]. Such methods have been actively developed during recent decades and are now a powerful tool for the evaluation of characteristics of complex low symmetry crystals. Different theoretical methods may be used for the calculations and several approaches were recently tested for an analysis of the electronic structure of chalcopyrites $LiAX_2$ (A = Al, Ga, In; X = S, Se, Te) [16–21]. Comparison of calculated characteristics, however, with experimental results presently available for $LiAX_2$ crystals is very limited, which restrains optimization of common theoretical models for this class of compounds. In this connection, the present study is aimed at using the plane-wave pseudopotential method based on density functional theory (DFT) for detailed evaluation of the band structure of LGS. The starting calculation process will be developed by comparison with valence band structure measured with x-ray photoelectron spectroscopy (XPS). After this, the dispersion of the optical parameters of LGS will be calculated and compared with the results obtained by spectroscopic ellipsometry.

2. Computational methods

In first-principles calculations, the plane-wave pseudopotential method [22] based on density functional theory [23] (DFT) has been used. The CASTEP program is employed to perform the electronic structure and the density-of-states (DOS) calculations [24]. Norm-conserving pseudopotentials are used with the 1s electrons for lithium and the 1s, 2s and 2p electrons for sulfur treated as core electrons [25]. For gallium, 3d, 4s and 4p electrons are chosen as the valence electrons. A well-converged kinetic-energy cutoff of 900 eV for plane-wave expansion is used. Monkhorst–Pack k-point meshes with a density of $(4 \times 3 \times 4)$ are chosen in the Brillouin zone of the LGS unit cell [26]. The general gradient approximation (GGA) with a PBE functional is employed here to describe the exchange–correlation interaction [27]. Although very successful for many systems of interest, the standard DFT method is well known to yield incorrect behavior of the electronic structure for materials which include elements containing d or f orbitals. The main reason for this is an absence of exactly solvable problems which can be used for parameterization of generalized exchange–correlation energy. So, a model must be created for this purpose. In this work we used the DFT + U method by explicitly adding an additional orbital-dependent (d-orbital-related) interaction, Hubbard U, to the Hamiltonian, thus giving improved results for the electronic states of the d orbitals [28, 29]. A detailed description of the Hubbard potential selected for LGS is presented below.

After obtaining the electronic structures, the transition rates between occupied and unoccupied states caused by the interaction with photons are determined. The imaginary part of the dielectric constant ε_2 can be described as a joint density of states between the valence and conduction bands, weighted by the appropriate matrix elements [30]:

$$\varepsilon_2(\hbar\omega) = \frac{2e^2\pi}{\Omega\varepsilon_0} \sum_{k,\mathrm{v,c}} |\langle\psi_k^{\mathrm{c}}|\hat{u}\cdot\vec{r}|\psi_k^{\mathrm{v}}\rangle|^2 \delta(E_k^{\mathrm{c}} - E_k^{\mathrm{v}} - \hbar\omega)$$

where Ω is a volume of the elementary cell, v and c represent the valence and conduction bands, respectively, k represents the k-point, ω is the frequency of the incident light and $\hat{u}$ is the vector defining the electric field polarization of the incident light, which is averaged over all spatial directions in the polycrystalline case. The optical absorption curve can be obtained directly from the imaginary part of the dielectric constant ε_2, while the refractive index dispersion curve can be obtained through the Kramer–Kronig transformation.

It is well known that the bandgap calculated by DFT is smaller than that obtained in experiments. This discrepancy appears due to the discontinuity of exchange–correlation energy. Therefore, a scissors operator was introduced to shift all the conduction levels up to agreement with the earlier measured value of the bandgap [31, 32].

3. Experimental methods

Bulk LGS crystal was grown on an oriented seed by the Bridgman–Stockbarger technique in a vertical set-up. Starting materials were Li of 99.9% purity and Ga, S—elementary components, which have been preliminarily purified to 99.999% level. All operations on growth experiment preparations were made inside a dry chamber. Particular

attention was paid to the composition of the starting charge, which has been corrected accounting for the incongruent sublimation. Since the volatile component S has a high partial vapor pressure at temperatures of LGS pyrosynthesis, the procedure was carried out in a two-region furnace to avoid a container explosion. The details of starting charge preparation and selection of optimal composition can be found elsewhere [6]. The temperature of a 'hot' region, where a crucible with the reaction mixture was placed, was 50–100 °C higher than the melting temperature of the growing crystal of about 1020 °C. The temperature of the 'cold' region was taken so that vapor pressure did not exceed 2 atm. Crystals were grown in a carbonglass crucible, located inside the silica ampule, whereas the latter was filled with Ar (1–1.5 atm.). Samples for XPS analysis and spectroscopic ellipsometry measurements were cut from the crystal part without visible defects. A plate for optical measurements was cut without control of the crystallographic orientation. The surface of the substrate was mechanically polished up to optical grade.

The x-ray photoemission spectra were obtained with a MAC-2 (RIBER) analyzer using nonmonochromatic Al Kα radiation (1486.6 eV) with a power of 300 W. This x-ray source was taken to minimize the effects of superposition of photoelectron and Auger lines of constituent elements. The diameter of the x-ray beam was ~5 mm. The energy resolution of the instrument was chosen to be 0.7 eV, so as to have sufficiently small broadening of natural core level lines at a reasonable signal–noise ratio. Under the conditions the observed full width at half-maximum (FWHM) of the Au $4f_{7/2}$ line was 1.31 eV. The binding energy (BE) scale was calibrated in reference to the Cu $3p_{3/2}$ (75.1 eV) and Cu $2p_{3/2}$ (932.7 eV) lines, assuming an accuracy of 0.1 eV in any peak energy position determination. Photoelectron energy drift due to charging effects was taken into account in reference to the position of the C 1s (284.6 eV) line generated by adventitious carbon on the surface of the powder as inserted into the vacuum chamber.

Spectral dependences of the refractive index $n(\lambda)$ and extinction coefficient $k(\lambda)$ were determined with the help of spectroscopic ellipsometry. Ellipsometric angles Ψ and Δ were measured as a function of λ in the photon energy range 1.2–5.0 eV (~250–1030 nm) using a Spectroscan ellipsometer. The instrumental spectral resolution was 2 nm, the recording time of a spectrum did not exceed 20 s and the angle of incidence of the light beam on the sample surface was taken as 70°. We used the four-zone method of measuring with subsequent averaging over all four zones. The ellipsometry data Ψ and Δ are related to the complex Fresnel reflection coefficients by the equation

$$tg\Psi e^{i\Delta} = \frac{R_p}{R_s}$$

where R_p and R_s are the coefficients for p-and s-polarized lightwaves, respectively. To calculate the dependences $n(\lambda)$ and $k(\lambda)$, the experimental data were processed using the model of an air–homogeneous isotropic substrate. Then the error function σ was minimized in the entire spectral range:

$$\sigma^2 = \frac{1}{m}\sum_{i=1}^{m}[(\Delta_{exp} - \Delta_{calc})^2 + (\Psi_{exp} - \Psi_{calc})^2]$$

where Δ_{calc}, Ψ_{calc} and Δ_{exp}, Ψ_{exp} are, respectively, the calculated and experimental ellipsometric angles and m is the number of points in the spectrum. The Lorentz–Drude approximation was used to fit the spectral dependences $\Psi(\lambda)$ and $\Delta(\lambda)$ and calculate the dispersion relations $n(\lambda)$ and $k(\lambda)$ [33, 34]:

$$\varepsilon(E) = \varepsilon_\infty - \frac{E_{1D}^2}{E^2 - iE_{2D}E} + \sum_{n=1}^{m}\frac{A_n E_n^2}{E_n^2 - E^2 + i\Gamma_n E_n E}$$

where ε_∞ is the value of ε at $E \to \infty$, the second term in this expression reflects the contribution of Drude free carriers, E is the photon energy in eV, and E_{1D} and E_{2D} are the constants. The interband transitions are described by the third Lorentzian term on the basis of damping harmonic oscillators and A_n, E_n and Γ_n are, respectively, the strength, energy and broadening function of the nth oscillator from the m oscillators used in the simulation [33].

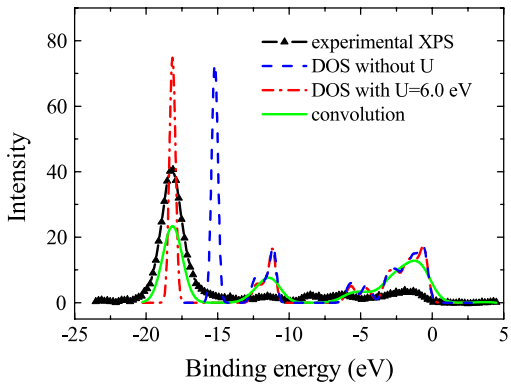

Figure 2. Valence band structure of $LiGaS_2$. The solid curve with triangles, dashed curve, dashed–dotted curve and solid curve represent the experimental XPS spectrum, the density of states (DOS) obtained from the standard DFT method, DOS obtained from the DFT + U method and the convolution of the calculated DFT + U DOS, respectively.

4. Results and discussion

In figure 2 the valence band structure measured for LGS with the XPS method is shown as a solid line with triangles. The peak of the Ga 3d levels is located at about −18.5 eV and has the largest intensity ever in the energy range −25–0 eV. For comparison, the DOS plot calculated by the standard DFT scheme is shown by a blue dashed line. It is evident that the location of the calculated Ga 3d states is about 3.5 eV higher than that of the experimental peak. This difference is generated, as mentioned above, due to the precision limit of the generalized exchange–correlation energy in the standard DFT scheme. In this work the discrepancy is corrected by using the DFT + U method. We found that, if the Hubbard U is taken as 6.0 eV, the location of Ga 3d states in the calculated DOS

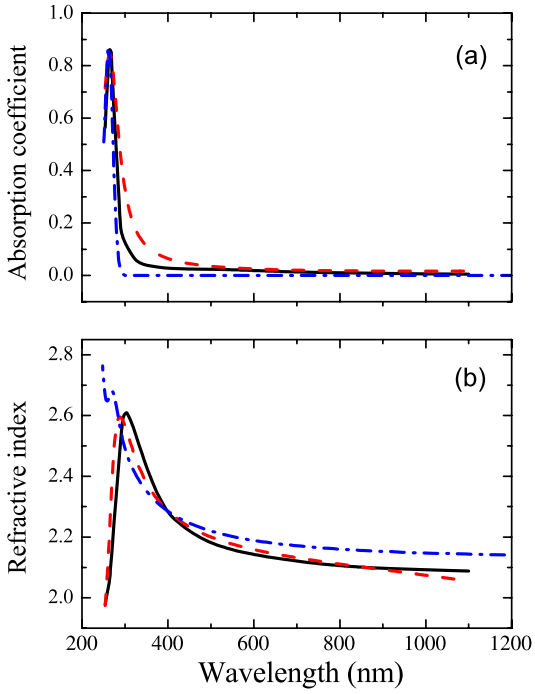

Figure 3. Dependences of (a) absorption coefficient and (b) refractive index of $LiGaS_2$ on the wavelength of incident radiation. Solid lines show the experimental data, dashed lines represent the simulation results using the Lorentz–Drude three-oscillator model and dashed–dotted lines represent the calculated results using the DFT + U method.

curve shown as a red dashed–dotted line in figure 2 is shifted to exact agreement with the Ga 3d peak measured with XPS. So this setting is used in the DFT + U calculations hereafter.

The calculated DFT + U DOS spectrum has very sharp components. A real XPS device, however, has limited spectral resolution and every sharp component is smoother in the measured spectrum. For the most accurate comparison, we make a convolution of the calculated DOS spectrum with the instrument function of our XPS device. As a result the green solid line in figure 2 is obtained. The energy position of spectral features in initial and transformed calculated spectra is the same but the components become wider. Generally, the transformed calculated spectrum is very similar to that measured in experiments except for the energy range of 5–9 eV. This discrepancy might be explained by the fact that in the pseudopotential method the electrons with energy deeper than the valence electrons are treated as core ones and these electronic orbitals are not displayed on the DOS spectrum.

The experimental dispersion curves obtained for the absorption coefficient and the refractive index of the LGS crystal are shown in figures 3(a) and (b), respectively, by red dashed lines. The dependences were measured with a spectroscopic ellipsometer for a polished LGS plate. This plate was cut without crystallographic control and the dependences may be classified as those related to the mean refractive index and mean absorption coefficient. Three oscillator Lorentz–Drude model was used for simulation. The parameters used for three-oscillator simulations are reported in table 1. A reasonable relation is found between the experimental curves

Table 1. Fitting parameters Lorentz–Drude approximation of $\Psi(\lambda)$ and $\Delta(\lambda)$ dependences.

Parameter	Value
ε_∞	2.597
E_{1D} (eV)	0.306
E_{2D} (eV)	15.794
A_1	1.985
E_1 (eV)	0.421
Γ_1 (eV)	0.156
A_2	0.672
E_2 (eV)	4.633
Γ_2 (eV)	0.179
A_3	1.202
E_3 (eV)	6.956
Γ_3 (eV)	0.05

and simulation results. Meanwhile, the absorption coefficient and refractive index of LGS are calculated as a function of energy with the DFT + U method and the curves are shown in figure 3 by blue dashed–dotted lines. To relate the calculated and experimental curves for the absorption coefficient shown in figure 3(a) the intensity of the maximum at about 4.7 eV was fitted to match the maximum in the experimental curve. It is revealed that the calculated absorption spectrum is excellently consistent with the experimental curve. As to refractive index dispersion (figure 3(b)), the calculated values are in good agreement with the experimental ones for low photon energies, but at higher energies the difference becomes noticeable. The difference may appear due to excitation of electrons from deeper orbitals that are not accounted in the model used for calculations.

5. Conclusions

The first-principles and experimental studies on the electronic and optical properties for the $LiGaS_2$ crystal are performed. Good agreement is found in the valence band structure measured with XPS and calculated with the first-principles pseudopotential method, except for the energy position of Ga 3d orbitals. The DFT + U method is employed to correct this discrepancy. As a result, the first-principles model is developed for calculation of physical properties of LGS. This model is tested in application to LGS optical constants. On the basis of electronic band structures, the optical absorption and mean refractive index of LGS were theoretically determined as a function of wavelength. The dispersive parameters are consistent with those carried out with spectroscopic ellipsometry. Due to the suitability and reliability the *ab initio* calculations and the spectroscopic ellipsometry method presented in this work will be jointly employed to study the properties of Li(In, Ga)S_2-doped crystals in future work.

Acknowledgments

The calculations were performed using high performance computing facilities at the Technical Institute of Physics and Chemistry, Chinese Academy of Sciences, PR China. ZSL acknowledges the support by the National Nature Science

Foundation of China (no. 50590402) and by the Special Foundation of President of The Chinese Academy of Sciences.

References

[1] Leal-Gonzalez J, Melibary S S and Smith A J 1990 *Acta Crystallogr.* C **46** 2017
[2] Isaenko L, Yelisseyev A, Lobanov S, Titov A, Petrov V, Zondy J-J, Krinitsin P, Merkulovm A, Vedenyapin V and Smirnova J 2003 *Cryst. Res. Technol.* **38** 379
[3] Isaenko L, Vasilyeva I, Merkulov A, Yelisseyev A and Lobanov S 2005 *J. Cryst. Growth* **275** 217
[4] Huang J-J, Atuchin V V, Andreev Yu M, Lanskii G V and Pervukhina N V 2006 *J. Cryst. Growth* **292** 500
[5] Isaenko L, Yelisseyev A, Lobanov S, Krinitsin P, Petrov V and Zondy J-J 2006 *J. Non-Cryst. Solids* **352** 2439
[6] Isaenko L I and Vasilyeva I G 2008 *J. Cryst. Growth* **310** 1954
[7] Atuchin V V, Kidyarov B I and Pervukhina N V 2006 *Comput. Mater. Sci.* **37** 507
[8] Kidyarov B I and Atuchin V V 2007 *Ferroelectrics* **360** 96
[9] Atuchin V V and Kidyarov B I 2007 *Ferroelectrics* **360** 100
[10] Reddy R R, Rama Gopal K, Narasimhulu K, Siva Sankara Reddy L, Raghavedra Kumar K, Krishna Reddy C V and Nisar Ahmed S 2008 *Opt. Mater.* **31** 209
[11] Korotkov A S and Atuchin V V 2008 *Opt. Commun.* **281** 2132
[12] Levine B F 1973 *Phys. Rev.* B **7** 2600
[13] Levine Z H 1990 *Phys. Rev.* B **42** 3567
[14] Levine Z H and Allan D C 1991 *Phys. Rev.* B **44** 12781
[15] Rashkeev S N and Lambrecht W R L 2001 *Phys. Rev.* B **63** 165212
[16] Bai L, Lin Z S, Wang Z Z and Chen C T 2008 *J. Appl. Phys.* **103** 083111
[17] Reshak A H, Auluck S, Kityk I V, Al-Douri Y, Khenata R and Bouhemadou A 2008 *Appl. Phys.* A **94** 315
[18] Li L-H, Li J-Q and Wu L-M 2008 *J. Solid State Chem.* **181** 2462
[19] Atuchin V V, Isaenko L I, Kesler V G, Lobanov S, Huang H and Lin Z S 2009 *Solid State Commun.* **149** 6
[20] Kosobutsky A V, Basalaev Yu M and Poplavnoi A S 2009 *Phys. Status Solidi* b **246** 364
[21] Reshak A H, Auluck S and Kityk I V 2009 *J. Alloys Compounds* **473** 20
[22] Payne M C, Teter M P, Allan D C, Arias T A and Joannopoulos J D 1992 *Rev. Mod. Phys.* **64** 1045
[23] Hohenberg P and Kohn W 1964 *Phys. Rev.* B **136** 864
[24] Clark S J, Segall M D, Pickard C J, Hasnip P J, Probert M, Refson J K and Payne M C 2005 *Z. Krystallogr.* **220** 567
[25] Lin J S, Qteish A, Payne M C and Heine V 1993 *Phys. Rev.* B **47** 4174
[26] Monkhorst H J and Pack J D 1976 *Phys. Rev.* B **13** 5188
[27] Perdew J P, Burke K and Ernzerhof M 1996 *Phys. Rev. Lett.* **77** 3865
[28] Cococcioni M and de Gironcoli S 2005 *Phys. Rev.* B **71** 035105
[29] Dudarev S L, Botton G A, Savrasov S Y, Humphreys C J and Sutton A P 1998 *Phys. Rev.* B **57** 1505
[30] Palik E D 1985 *Handbook of Optical Constants of Solids* (Orlando: Academic)
[31] Godby R W, Schluter M and Sham L J 1988 *Phys. Rev.* B **37** 10159
[32] Wang S and Klein B M 1981 *Phys. Rev.* B **24** 3417
[33] Postava K, Aoyama M and Yamaguchi T 2001 *Appl. Surf. Sci.* **175** 270
[34] Langereis E, Heil S B S, Knoops H C M, Keuning W, van de Sanden M C M and Kessels W M M 2009 *J. Phys. D: Appl. Phys.* **42** 073001